Sławomir JURKOWSKI[1], **Józef CIUŁA**[2]

[1] University of Applied Sciences in Nowy Sącz, Faculty of Engineering Sciences, Zamenhofa 1a, 33-300 Nowy Sącz, e-mail: sjurkowski@ans-ns.edu.pl
[2] University of Applied Sciences in Nowy Sącz, Faculty of Engineering Sciences, Zamenhofa 1a, 33-300 Nowy Sącz, email: jciula@ans-ns.edu.pl

The use of rapid prototyping methods and FEM analyses to improve aerodynamic characteristics of passenger vehicles

Abstract

The aerodynamic features of motor vehicles mainly affect two aspects: operating costs related to the drag force of the vehicle (Cx coefficient) and traction properties. The simulation tests carried out made it possible to modify body elements in order to improve the aerodynamic downforce of the rear axle of the vehicle and to evaluate the range of rear spoiler settings from the point of view of its usefulness. The research problem was the analysis of the aerodynamic features of the BMW E46 325i vehicle, based on CFD numerical analyses and the design of an active spoiler. The body of the vehicle was digitized on the basis of a point cloud using the Smarttech3D Universe optical scanner and the SpaceClaim program from the ANSYS package. Numerical calculations were carried out in the vehicle speed range of 50-245 [km/h]. Air streams flowing around the body of the vehicle were analysed. The dynamically designed rear spoiler has three positions relative to the boot lid: 0°, 10° and 20°. The analysed range of speeds and spoiler angles allowed to determine the aerodynamic downforce and the active spoiler control map, i.e. the extension of the positioning mechanism and setting the angle of the system relative to the plane of the trunk depending on the speed of the vehicle. The aerodynamic downforce ranged from 0.5 to 321 [N]. Based on the data obtained, it was found that the factory body geometry provides aerodynamic downforce of 3 to 93 [N], the use of a spoiler increases this value from 12 to 228 [N], with a decrease in the Cx coefficient from 1 to 3 [%]. The beneficial effect of using a spoiler is registered above the speed of 50 [km/h], and the optimum angle of attack of the spoiler is 10°.

Keywords: FEM, FVM, ANSYS, aerodynamics, vehicle, Cx, down force.

Zastosowanie metod szybkiego prototypowania i analiz MES do poprawy charakterystyk aerodynamicznych pojazdów osobowych

Streszczenie

Cechy aerodynamiczne pojazdów samochodowych wpływają głównie na dwa aspekty: koszty eksploatacji związane z siłą oporu powietrza (współczynnik Cx) i właściwości trakcyjne. Przeprowadzone testy symulacyjne umożliwiły modyfikację elementów nadwozia w celu poprawy siły docisku aerodynamicznego tylnej osi pojazdu oraz ocenę zakresu ustawień tylnego spoilera pod kątem ich użyteczności. Problem badawczy stanowiła analiza właściwości aerodynamicznych samochodu BMW E46 325i na podstawie analiz numerycznych CFD i projekt aktywnego spoilera.

Nadwozie pojazdu zostało zdigitalizowane na podstawie chmury punktów przy użyciu optycznego skanera Smarttech3D Universe oraz programu SpaceClaim z pakietu ANSYS. Obliczenia numeryczne przeprowadzono w zakresie prędkości pojazdu od 50 do 245 km/h, analizując przepływ strug powietrza wokół karoserii. Dynamicznie zaprojektowany tylny spoiler posiada trzy pozycje względem pokrywy bagażnika: 0°, 10° i 20°. Analizowany zakres prędkości i kątów nachylenia spoilera pozwolił określić wartości docisku aerodynamicznego oraz opracować mapę sterowania aktywnym spoilerem, obejmującą wysuw mechanizmu pozycjonującego i ustawienie kąta systemu względem płaszczyzny bagażnika w zależności od prędkości pojazdu.

Uzyskana siła docisku aerodynamicznego mieściła się w zakresie od 0,5 do 321 N. Na podstawie uzyskanych danych stwierdzono, że fabryczna geometria nadwozia generuje docisk aerodynamiczny od 3 do 93 N, natomiast zastosowanie spoilera zwiększa tę wartość do 12-228 N, przy jednoczesnym spadku współczynnika oporu Cx o 1-3%. Korzystny wpływ spoilera odnotowano przy prędkościach powyżej 50 km/h, a optymalny kąt jego nachylenia określono na 10°.

Słowa kluczowe: MES, FVM, ANSYS, aerodynamika, pojazd, Cx, siła docisku.

1. Introduction

Rapid prototyping is a technology that supports the work of modern engineers. Its basic design process includes rapid prototyping of models with appropriate geometry, data conversion and final processing (including verification). Applying 3D scanning involves collecting digital data about the shape and appearance of real objects to create digital models (Hyndhavi, Murthy, 2017). Rapid prototyping methods are also used in design work in industries that produce equipment that converts renewable energy into other forms of energy. This concerns hydropower (water turbines), biogas and biomass in combined heat and power plants (gas turbines and steam turbines) and, in particular, wind power in the blade area of wind turbines to determine the aerodynamic profile of the wind turbine. Comparison of the blade structure and its mechanical strength with the loads occurring during operation (Poole, Phillips, 2019; Ciuła et al., 2023). The process used to manufacture wind turbine blades consists of various steps, including: CAD model development procedures and 3D printing processes, printing of turbine blade geometries (enhanced production) and reinforcement of the blade structure (Bassett et al., 2015). To optimize rapid prototyping processes, virtual reality systems are increasingly used to model these processes. Such measures are intended to reduce the risks associated with prototype production in the early stages of the product development cycle. Therefore, by applying modeling and simulation in virtual systems, we reduce the number of prototyping, building, testing and testing cycles (Choi, Samavedam, 2022).

Another area related to rapid prototyping is the acquisition of input data for computational processes and the use of incremental manufacturing methods. This is especially true for three-dimensional models of real objects, such as prototype structures, objects without design documentation, or components that have been damaged and need to be rebuilt (Kowalski et al., 2022). One method of obtaining a three-dimensional model is so-called drawing from nature, which involves measuring the geometric properties of elements and then drawing the object in a CAD program. This method is commonly used in manufacturing facilities for design purposes with incomplete input data sets. A significant problem arises with objects with irregular shapes and elements that are difficult to describe using simple geometric blocks. In this case, the scanning method is still available. As basic methods of 3D scanning (Confalone et al., 2023) we can distinguish: contact method, laser (triangulation and ToF), stereo, photogrammetry, structural light scanning and computer tomography (Olejarczyk et al., 2020). In the case of incremental manufacturing methods, the most important aspect is to obtain on the basis of the cloud points a model free of discrepancies and anomalies caused by measurement errors (Rosso et al., 2020). The finite element method also requires the even distribution of the grid of triangles from which the 3D model is constructed. The size and shape of the triangles forming the surface of the object, and errors associated with uncovered surfaces, duplicated edges, etc., are crucial when working grid algorithms. These types of errors in a three-dimensional model cause the object to be divided into finite elements of low quality, which consequently increases the number calculation errors. Today, rapid prototyping methods are closely related to numerical methods, including the finite element method (FEM) (Cui, 2015). On the one hand, some numerical analyses require the import of CAD models of physical objects, on which strength, heat, flow, etc. are calculated. There is also a dependency: the results of the numerical analysis provide the basis for the redesign of the object of investigation and the empirical verification of whether the basic goals of the redesign are achieved (Pawłucki, 2015). Additive production methods can be used here (Szczepaniak et al., 2015).

2. Materials and methods

The aerodynamic characteristics of motor vehicles are mainly affected by two aspects: the operating costs associated with the vehicle's drag force (coefficient C_x) (Piechna, 2012) and with the traction properties (Gao, Xin, 2021; Anderson, 2010). The simulation studies allowed the body components to be modified to improve the aerodynamic strain on the rear axle (Katz, 1985) of the vehicle and to assess the range of rear spoiler settings (Somerfield, 2023) from the point of view of its usability (Rohl et al., 1995). Modelling of turbulent flows around moving vehicles makes it possible to analyse the correctness of determining the geometric characteristics of aerodynamic elements (Paszko, Łygas, 2016), similar analyses are being carried out on a large scale in the field of aviation (Yurkovich, 2003). The characteristics of vehicle geometry also have a significant impact on emissions of pollutants into the atmosphere, which is emphasized by (Ciuła et al., 2019; Generowicz et al., 2019).

Technical capabilities of the 3D Printing Laboratory and the Metrological Laboratory of the University of Applied Sciences in Nowy Sącz have the possibility of contact scanning using a coordinate measuring arm. Photogrammetric methods are implemented by systems based on the software Photoscan and Zephyr 3DF. In addition, the Department of Engineering Sciences is equipped with the David SLS 2 and Smarttech Universe systems for structural light scanning. For the purposes of rapid prototyping and FEM analysis, the data obtained i.e. the cloud of points identified on the surface of the measured object requires additional processing for its later use. The technical facilities of the Faculty of Engineering Sciences in this regard allow the use of both basic, commonly available methods of incremental production, such as FDM (Fused Deposition Modeling), as well as advanced technologies SLA (Stereolitography) (Yurkovich, 2003) and SLS (Selective Laser Sintering) (Tuliszka-Sznitko, 2011) and numerical calculations using the method of finite elements FEM in the ANSYS package. Numerical analyses allow for the reduction of the number of prototypes made during the redesign phase, which impacts the reduction of waste production, thus making a significant contribution to environmental protection (Przydatek et al., 2017; Kochanek, Kobylarczyk, 2024). Such an approach aligns with the idea of sustainable development described, among others, by (Kochanek et al., 2024).

The research problem was the analysis of the aerodynamic characteristics of the BMW E46 325i, based on numerical CFD analyses and the design of the active spoiler (Vreman et al., 1997). The vehicle was digitized on the basis of the point cloud using the Smarttech3D Universe optical scanner. The car body is an object that is relatively difficult to digitize with a scanner operating in structural light technology. Painted elements, chrome elements and glazing generate reflections of Gray codes, displayed by the thrower on the vehicle's surface, as a result of which the detector captures a blurred, inaccurate image of the surface. The measurement area recorded with one fixing of the scanner is effectively 300 mm per 250 mm, which in combination with large surfaces of body components, such as roof, front mask, or windows makes it difficult to impose on each other further clouds of points (no characteristic transitional elements) (Park, Kwon, 1996). In order to improve the quality of the obtained clouds of dots, the vehicle's coil is covered with a trigger used in welding for testing non-destructive bonds. In addition, the number of shots required for capturing was limited by measuring only on the right side of the car. The CAD model was obtained by copying the resulting cloud of points, making a mirror reflection, and attaching the resulted object to the original cloud. The processing of the obtained data consisted of cleaning the scans from the interference and unwanted elements that were accidentally identified, by mutually adjusting the resulting clouds, based on the characteristic points identified on the adjacent images. The CAD model building algorithm reduces the number of measurement points taken into account when determining the triangle grid, in this case a reduction of 10%. The obtained 3D model is saved in .stl format. For the purposes of producing a model on a scale using incremental methods, the model proved to be satisfactory. In the case of FEM analyses, geometry errors made it impossible to divide the object into finite elements, it was necessary to use the Space Claim program from the ANSYS package, the final effect of the work on the reproduction of the car's body is shown in Figure 1. The model optimization for numerical analysis was based on the regularization of the triangle grid, the reduction of the disproportions in the dimensions of the 3D model grid-building triangles, and the use of geometry error detection algorithms for FEM calculations (Iljaszewicz et al., 2020).

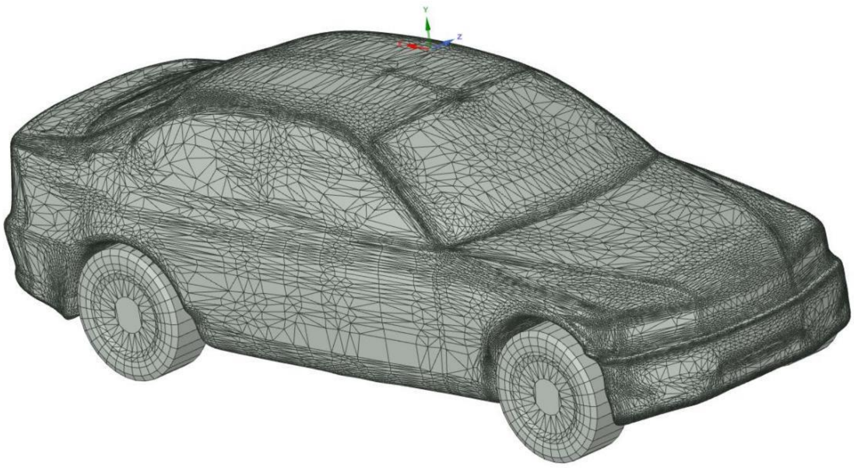

Figure 1. The three-dimensional model of the BMW E4

(source: own study)

The FEM flow analysis system was based on ANSYS software. A view of the calculation modules used in performing the calculations is shown in Figure 2. The three-dimensional model was imported using the Geometry module marked as A in Figure 2. Modules from B to I are flow analysis computing environments based on the Fluent meter.

The calculations were made on the factory geometry of the vehicle (modules B and G), on the vehicle equipped with the rear spoiler adjusted at angles of 10° (Modules C and H) and 20° (Modules D and I). The calculations were made for two turbulence models: kε and kω (Arrondeau, Rana, 2020). Due to the convergence of results obtained with different turbulence models, the article presents data for the kε model with turbulence determine by intensity and hydraulic diameter with turbulence intensity set up as 5%. In another articles we find the same turbulence models, and conclusion that kω SST model can by better in more complex flow cases (Czyż et al., 2018).

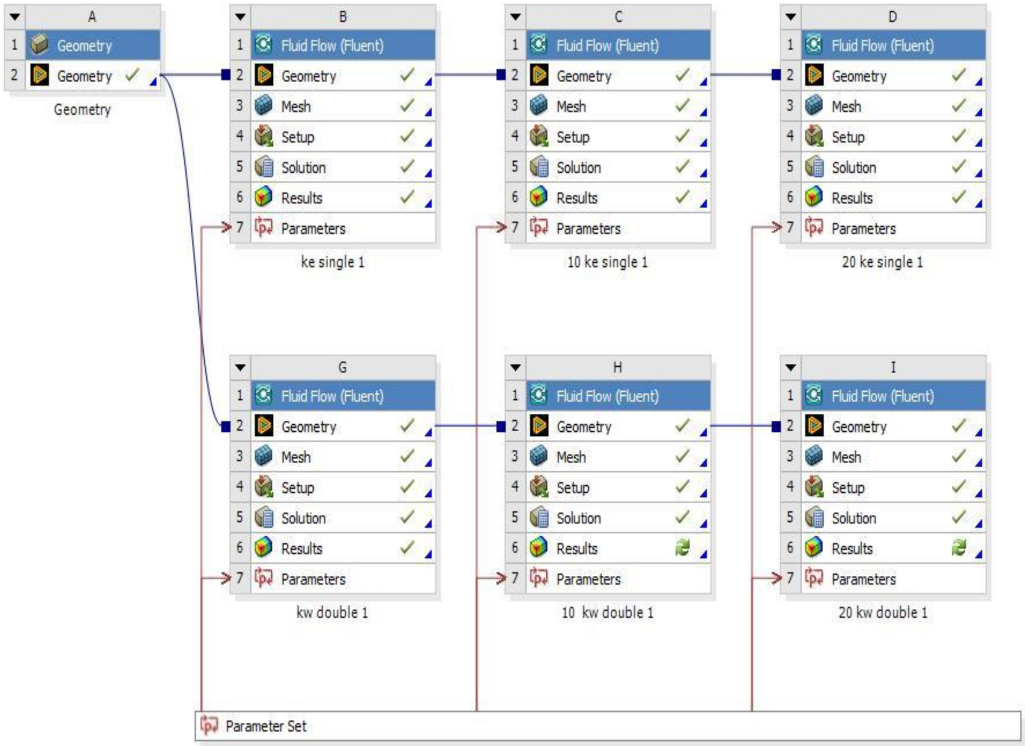

Figure 2. A connections of analysis systems in ANSYS Workbench

(source: own study)

The red arrow indicates the input data that controls the calculations, stored in the Parameter Set module (Sangeetha, 2015). In this case, the input parameter was the air flow speed of the car, for the full range of reachable speeds, in this case: 50; 100; 150; 200; 245 [km/h]. We can find another calculation with a range of vehicle speed between 20 and 325 [km/h] (Czyż et al., 2018), but in this case the lower speed is similar to the cited research, and the maximum speed is equal to the maximum reachable speed of the BMW 325i.

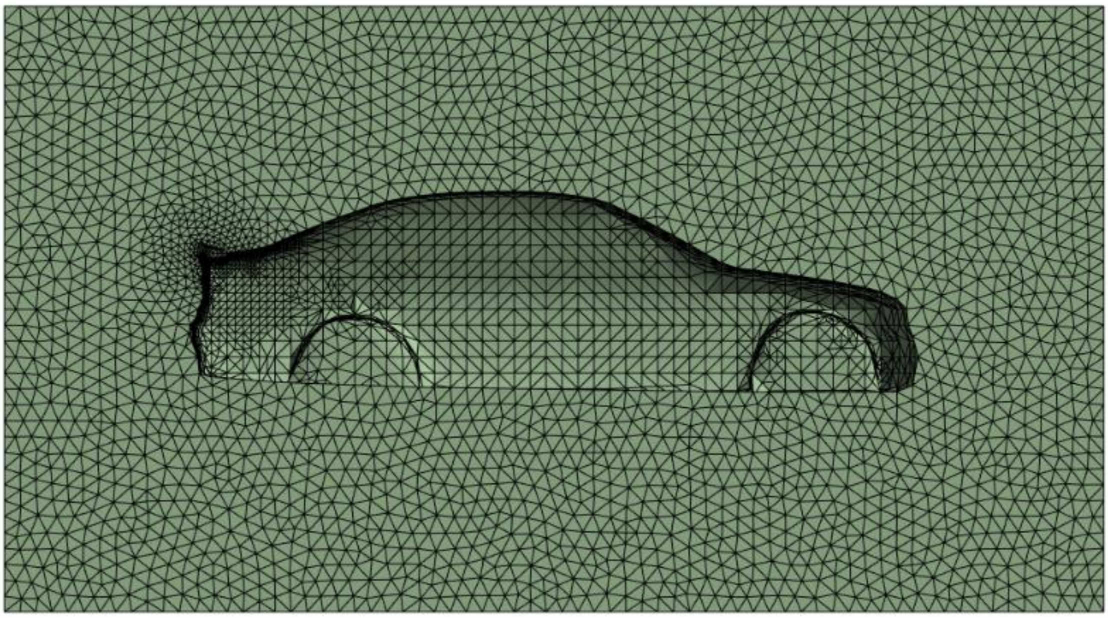

Figure 3. Divide a domain into finite elements

(source: own study)

The results after the meshing process are shown in Figure 3. We set the maximum finite element size to 72 [mm] during grid generation and enabled the grid thickening function at the Curvature Minimum Size of 4.5 [mm]. We introduced the speed of the gas through the "inlet" wall within the Parameter Set range of 50-245 [km/h]. We expanded the computing domain by 1 [m] in each direction, taking into account the vehicle dimensions. In order to limit the required measuring power, half of the model was reduced along the symmetrical plane. The minimum element quality parameter is about 0.13. There are 480092 elements, and 86873 nodes were obtained. The calculation was made with a pressure base type and steady-state conditions. It was assumed that the medium was the ideal gas (air), with a viscosity of $1.7894 \cdot 10^{-5}$ [$kg \cdot m^{-1} \cdot s^{-1}$] and a temperature of 15 [°C].

3. Results and discussion

The calculations allowed to generate flowing air strands of the geometry analysed, a representative example is shown in Figure 4. The turbulence that occurs around the vehicle can be observed visually, in addition each of the straws represents the speed of air flow represented by the colour scale.

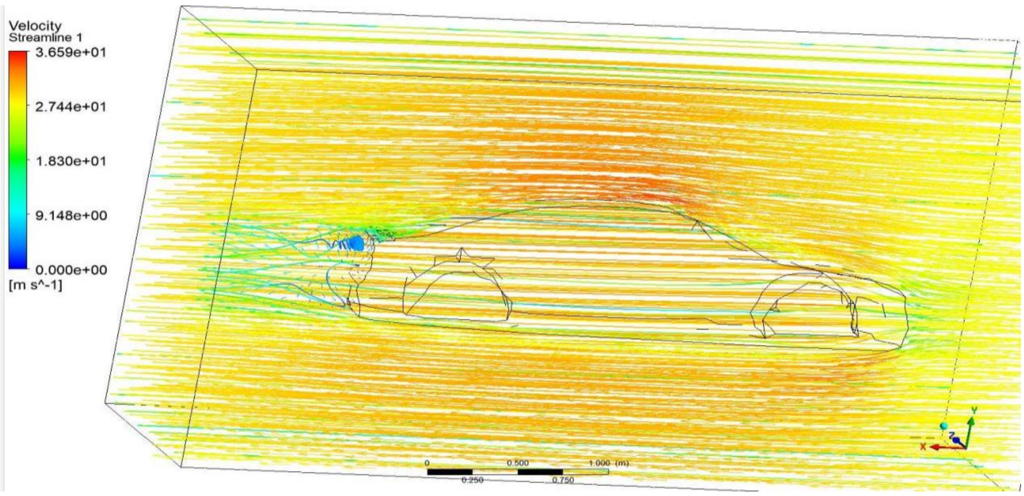

Figure 4. Visualization of air stream lines flowing through the car

(source: own study)

A visual analysis of the air strands provides the basis for determining the best position of the rear spoiler to efficiently utilize the kinetic energy of the gas. The case shown in Figure 3 indicates that the spoiler should be raised slightly in relation to the current position at the prototype stage so that a higher-speed air pipe is on the way. The analysis of the forces acting on the vehicle resulting from its aerodynamic characteristics was carried out separately for the horizontal component (the resistance force acting along the calculated axis X) and the vertical (the force of the aerodynamic pressure, operating along the axis Y). A summary of resistance data is provided in Figure 1 for three cases:

- 0° – the vehicle's factory edge (spoiler case from resting position – counting with the trunk lid);
- 10° – a spoiler in working position with an angle of impact setting of 10° in relation to the plane of the tray lid;
- 20° – a spoiler at work position with a angle of stress setting of 20° in respect of the surface of the luggage lid.

Additionally, a graph of the dependency of the resistance force on the speed of the vehicle is drawn up and is shown in Figure 5 and Table 1. It can be noticed that slight differences in resistance were obtained at angles 0° and 10°, only at a larger angle of impact the resistance begins to increase significantly. From the economic point of view, setting the spoiler at an angle of about 10° gives the best results. Further analysis should be carried out for more impact angle settings. The data obtained will be used to develop a map of the device control.

Table 1
Drag force calculated using FEM for the variable angle of the spoiler slope and different vehicle speeds

	Force of aerodynamic Resistance [N]		
	Spoiler angle		
Velocity [km/h]	**0°**	**10°**	**20°**
50	20.20	20.68	28.83
100	82.47	79.95	101.54
150	178.46	177.53	226.77
200	316.35	314.41	403.16
245	472.92	470.25	599.29

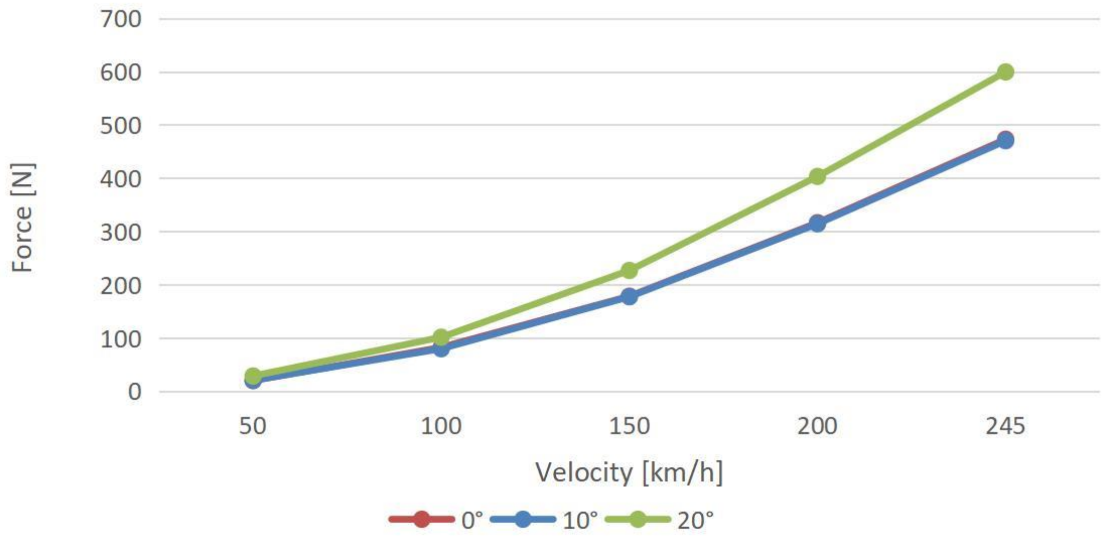

Figure 5. Dependency of drag force on vehicle speed

Table 2
Drag force calculated using FEM for the variable angle of the spoiler slope and different vehicle speeds

Force of aerodynamic resistance [N]			
Spoiler angle			
Velocity [km/h]	**0°**	**10°**	**20°**
50	-1.73	-7.54	-3.57
100	-0.26	-29.38	-17.84
150	-15.67	-63.42	-40.54
200	-28.76	-144.07	-70.26
245	-46.78	-160.51	-104.27

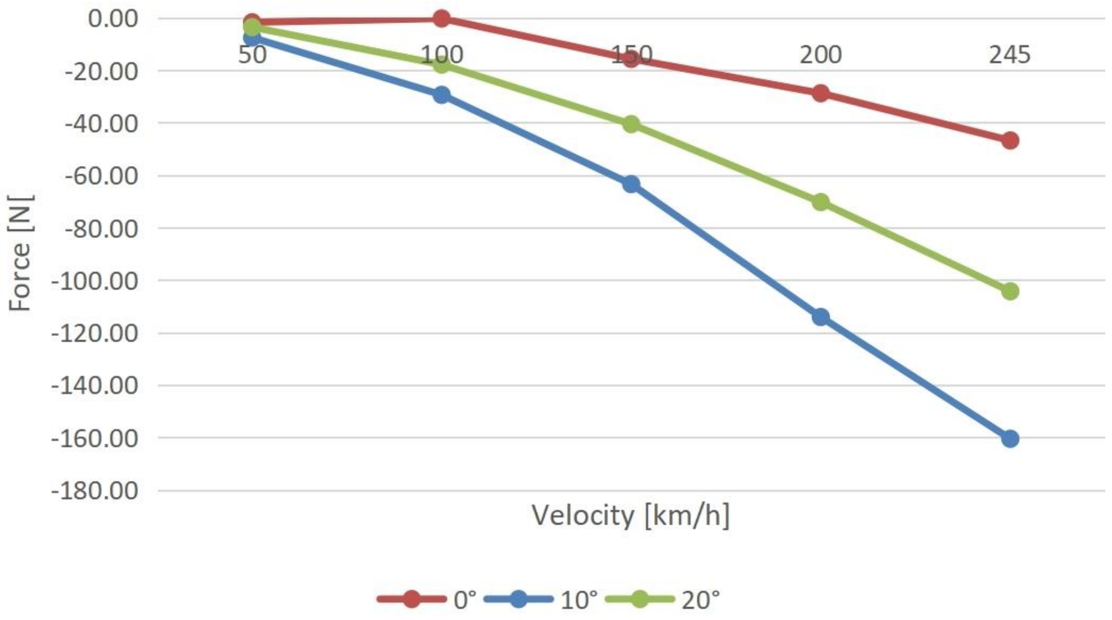

Figure 6. The impact of the aerodynamic pressure force from the spoiler impact angle

In addition, a graph of the relationship of the aerodynamic pressure force to the speed of movement of the vehicle is produced and is shown in Figure 6. It can be noticed that an increase in the force of aerodynamic pressure has already been achieved from the setting of the spoiler at an angle of 10°, while at the same time a slight increase in srag force (Figure 5), which confirms that this is the most reasonable area of the device settings. Changing the geometry of the body affects the change in the air resistance factor, this factor has a direct effect on the strength of the drag force. Car body designers, on the one hand, take into account the visual qualities, and on the other hand, the movement resistors of the vehicle, which in half make up the aerodynamic resistors (Dadbakhsh, 2017). Formula 1 allows you to calculate the strength of the drag force.

$$F_p = 0{,}5 \cdot A \cdot V^2 \cdot C_x \cdot \rho \quad (1)$$

Where: F_p – drag force, ρ – air density depending on temperature and pressure, V – object velocity, A – front surface of the car, C_x – air resistance coefficient. Having the data on air resistance, the resistance factor C_x was calculated for the original body of the vehicle and for the geometry of the working spoiler. The calculations were performed using formula 2.

$$C_x = \frac{F_p}{0{,}5 \cdot A \cdot V^2 \cdot \rho} \quad (2)$$

Table 3 summarizes the percentage change in the drag force factor. For the impact angle of 10° for low speeds the coefficient has deteriorated by 2.4 [%] while at speeds of about 100 [km/h] we record an improvement of the resistance factor by 3.1 [%]. By increasing the speed the change factor is negligible. At an impact angle of 10°, a significant deterioration of the C_x factor is observed, reaching 42.7 [%] at a speed of 50 [km/h].

Table 3
Change of the Cx factor calculated for the variable angle of the spoiler inclination and the different speeds of the car

Changing the C_x coefficient		
Spoiler angle		
Velocity [km/h]	**10°**	**20°**
50	2,4%	42.7%
100	-3.1%	23.1%
150	-0.5%	27.1%
200	-0.6%	27.4%
245	-0.6%	26.7%

The simulation studies were extended to include strength analyses carried out to confirm the possibility of using additive manufacturing methods in the manufacture of the rear spoiler prototype. The manufacturing technology that has been taken into account is selective plastics powder compression (SLS) (Pavan, 2017). The final manufacturing process will be carried out on the Sinterit Lisa Pro 2 device, which uses PA-12 polyamide as one of the available materials, characterized by the parameters set out in Table 4. Scientific research confirms the technical usefulness of components produced in addition to laser sintered Pa-12 powders (Yu et al., 2022). Parts made of this material are characterized by profound mechanical and tribological properties (Lammens et al., 20117; Razaviye et al., 2022).

Table 4
Plastic PA-12 material parameters

Parameter	**Value**	**Unit**
Density	21140	$kg \cdot m^{-3}$
Stretch strength	43	MPa
Elasticity module	2.2	GPa
Extension at breakdown	16-18	%
Hardness	75	Shore D

The results of the strength tests are shown in Figure 7. The maximum stress calculated according to von Misses' exhaust theory is 0,55 [MPa], which proves that the PA-12 material has mechanical properties (Tomanik et al., 2022) allowing for the manufacture of a fully functional prototype allowing the transfer of loads acting on the spoiler during operation of the vehicle throughout the available range of achieved speeds (Jurkowski, Janisz, 2019).

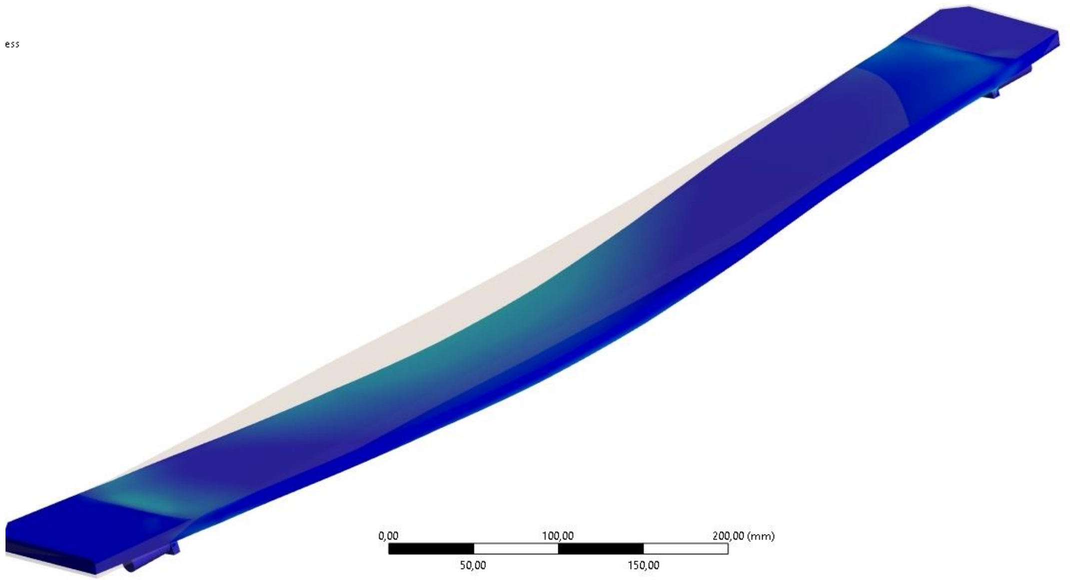

Figure 7. Stress map

The result differs significantly from the stretch strength of the material, which suggests the possibility of reducing the weight of the structure (material savings) while maintaining satisfactory strength properties. The Structural Optimisation module was used for this purpose, the software settings set the permissible weight reduction of the element to 50 [%] and the limit of computational iterations to 500. The results of the algorithm are shown in Figure 8. The resulting geometry forms the core of the structure (72,33 [%] of the output weight), carrying the loads, the remaining space can be supplemented with structures with empty spaces, e.g. with the structure of a honey plate, covered from the outside with a thin surface, preserving the aerodynamic and visual characteristics of the object.

Figure 8. Design with reduced volume

The results of the numerical tests confirm the validity of supplementing the vehicle's body with a spoiler providing the aerodynamic pressure of the rear axle, the use of FEM calculation methods has also provided information confirming the possibility of using quick prototyping methods in constructing a fully functional device that can be mounted in the vehicle.

4. Further directions of research

Preliminary research has allowed to determine the working area of the active rear spoiler that can be mounted in the BMW E46. Further stages of work include:

- FEM analyses aim to adjust the spoiler's geometry to increase aerodynamic pressure, which includes selecting the optimal surface and determining the spoiler's output beyond the vehicle's outline while considering the driving speed.
- the design of the exit mechanism and the angle of the inclination of a spoiler are important considerations.
- the project involves the installation of control and execution systems.
- creation of a map that shows the settings of the spojler based on the vehicle's speed;
- we are performing a fatigue analysis of the spoiler structure under variable conditions of the loads recorded during the vehicle's operation, using a methodology similar to the fatigue analyses of machine parts (Bajerlein et al., 2020).

5. Conclusions

Numerical calculations in the range of vehicle speed 50-245 [km/h] are similar to cited articles. The procedures and settings adhere to the same principles as those in analogy research. The air flows flowing through the vehicle were analyzed. The engineered rear spoiler, dynamically changing its position in relation to the car's body, is positioned in three positions relative to the luggage compartment: 0°, 10°, and 20°. The analyzed speed range and angles of the spoiler setting allowed the determination of the force of aerodynamic pressure and the map of the control of the active spoiler, i.e., the push of the positioning mechanism and the setting of the angle of the system relative to the plane of the trunk depending on the speed of movement of the vehicle. The force of aerodynamic pressure ranged from 0.5 to 321 [N]. Based on the data obtained, it was determined that the factory geometry of the body provides an aerodynamic pressure ranging from 3 to 93 [N]. The use of a spoiler increases this value from 12 to 228 [N] with a decrease of the C_x factor from 1 to 3 [%]. The beneficial effect of using a spoiler is recorded above a speed of 50 [km/h], and the optimal angle of the spoiler's impact is 10°. The use of rapid prototyping methods allows using the market-available PA-12 material to produce a fully functional prototype of the active spoiler. The optimization module, available in the ANSYS package, reduces the mass of the material used to about 72 [%], while maintaining the strength and useful characteristics of the object.

References

Anderson, J.D. Jr. (2010). *Fundamentals of Aerodynamics*. Tata McGraw-Hill Education: New York.

Arrondeau, B., Rana, Z.A. (2020). Computational Aerodynamics Analysis of Non-Symmetric Multi-Element Wing in Ground Effect with Humpback Whale Flipper Tubercles. *Fluids, 10*(5), 247. DOI: https://doi.org/10.3390/fluids5040247.

Bajerlein, M., Bor, M., Karpiuk, W., Smolec, R., Spadlo, M. (2020). Strength analysis of critical components of high-pressure fuel pump with hypocycloid drive. *Bulletin of the Polish Academy of Sciences, Technical Sciences, 68*, 1341-1350. DOI: https://doi.org/10.24425/bpasts.2020.135380.

Bassett, K., Carriveau, R., Ting, D.S.K. (2015). 3D printed wind turbines part 1: Design considerations and rapid manufacture potential. *Sustain. Energy Technol. Asses, 10*(11), 186-193. DOI: https://doi.org/10.1016/j.seta.2015.01.002.

Choi, S.H., Samavedam, S. (2022). Modelling and optimisation of Rapid Prototyping. *Computers in Industry, 10*(47), 39-53. DOI: https://doi.org/10.1016/S0166-3615(01)00140-3.

Ciuła, J., Gaska, K., Iljuczonek, Ł., Generowicz, A., Koval, V. (2019). Energy efficiency economics of conversion of biogas from the fermentation of sewage sludge to biomethane as a fuel for automotive vehicles. *Architecture Civil Engineering Environment ACEE, 2*, 131-140.

Ciuła, J., Kowalski, S., Generowicz, A., Barbusiński, K., Matuszak, Z. Gaska, K. (2023). Analysis of Energy Generation Efficiency and Reliability of a Cogeneration Unit Powered by Biogas. *Energies, 10*(16), 2180. DOI: https://doi.org/10.3390/en16052180.

Confalone, C.G., Smith, J. Kinnare, T. (2023). 3D Scanning for Advanced Manufacturing, Design, and Construction Wiley Sons. DOI: https://doi.org/10.1002/9781119758532.

Cui, G. (2015). Shape Optimization Based on ANSYS. *Journal of Information and Computational Science, 12*(11), 4291-4297. DOI: https://doi.org/10.12733/jics20106234.

Czyż, Z., Karpiński, P., Gęca, M., Diaz, J.U. (2018). The air flow influence on the drag force of a sports car. *Advances in Science and Technology Research Journal, 12*(2), 121-127. DOI: https://doi.org/10.12913/22998624/86213.

Czyż, Z., Karpiński, P., Sevdim, T. (2018). Numerical analysis of the drag coefficient of a motorcycle helmet. *Applied Computer Science, I*(1), 16-26. DOI: https://doi.org/10.23743/acs-2018-02.

Dadbakhsh, S., Verbelen, L., Verkinderen, O., Strobbe, D., Van Puyvelde, P., Kruth, J.P. (2017). Effect of PA12 powder reuse on coalescence behaviour and microstructure of SLS parts. *Eur. Polym. J., 10*(92), 250-62. DOI: https://doi.org/10.1016/j.eurpolymj.2017.05.014.

Gao, W., Xin Xin, K. (2021). Review of state of the art in active aerodynamic control research for vehicles. *Journal of Physics Conference Series*. DOI: https://doi.org/10.1088/1742-6596/1985/1/012040.

Generowicz, A., Kowalski, Z., Kulczycka, J., Banach, M. (2011). Assessment of technological solutions of municipal waste management using technology quality indicators and multicriteria analysis. *Przemysł Chemiczny, 90*/5, 747-753.

Hyndhavi, D., Murthy, S.B. (2017). Rapid Prototyping Technology – Classification and Comparison. *Int. Res. J. Eng. Tech., 10*, 43107-3111.

Iljaszewicz, P., Łusiak, T., Pastuszak, A., Novak, A. (2020) Aerodynamic analysis of the aircraft model made with the 3D printing method Transp. *Res. Procedia., 10*(51), 118-133. DOI: https://doi.org/10.1016/j.trpro.2020.11.014.

Jurkowski, S., Janisz, K. (2019). Analiza wpływu parametrów siatki obliczeniowej na wynik symulacji przepływomierza. Autobusy. DOI: https://doi.org/10.24136/atest.2019.238.

Katz, J. (1985). *Calculation of the Aerodynamic Forces on Automotive Lifting Surfaces ASME J. Fluids Eng*. DOI: https://doi.org/10.1115/1.3242507.

Kochanek, A., Ciuła, J., Generowicz, A., Mitryasova, O., Jasińska, A., Jurkowski, S., Kwaśnicki P. (2024). The Analysis of Geospatial Factors Necessary for the Planning, Design, and Construction of Agricultural Biogas Plants in the Context of Sustainable Development. *Energies, 17*, 5619. DOI: https://doi.org/10.3390/en17225619.

Kochanek, A.J., Kobylarczyk, S. (2024). Analiza głównych czynników geoprzestrzennych z wykorzystaniem programów geoinformacyjnych niezbędnych do planowania, projektowania i budowy elektrowni fotowoltaicznej. *J. Ecol. Eng., 25*, 49-65.

Kowalski, S., Opoka, K., Ciuła, J. (2022). Analysis of the end-of-life the front suspension beam of a vehicle. *Eksploatacja i Niezawodność – Maintenance and Reliability, 10*(24), 446-454. DOI: https://doi.org/10.17531/ein.2022.3.6.

Kurec, K., Remer, M. (2019). Advanced Modeling and Simulation of Vehicle Active Aerodynamic Safety. *Journal of Advanced Transportation*. DOI: https://doi.org/10.1155/2019/7308590.

Lammens, N., Kersemans, M., De Baere, I. Van Paepegem, W. (2017). On the visco-elasto-plastic response of additively manufactured polyamide-12 (PA-12) through selective laser sintering. *Polym. Test, 10*(57), 149-55. DOI: https://doi.org/10.1016/j.polymertesting.2016.11.032.

Olejarczyk, M., Gruber, P., Ziólkowski, G. (2020). Capabilities and limitations of using Desktop 3D printers in the laser sintering process. *Appl. Sci, 10*(10) 6184. DOI: https://doi.org/10.3390/app10186184.

Park, T.S., Kwon, J.H. (1996). An improved multistage time stepping for second-order upwind TVD schemes Comput. *Fluids, 10*(25),629-645. DOI: https://doi.org/10.1016/0045-7930(96)00014-X.

Paszko, M., Łygas, K. (2016). Współczesne metody modelowania przepływów turbulentnych w otoczeniu poruszającego się autobusu miejskiego. *Autobusy, 17*(12), 1269-1272.

Pavan, M. (2017). On the influence of inter-layer time and energy density on selected critical--to-quality properties of PA12 parts produced via laser sintering. *Polym Test, 10*(61), 386-395. DOI: https://doi.org/10.1016/j.polymertesting.2017.05.027.

Pawłucki, M. (2015). Multiple objective shape optimization in Ansys Fluent Solver. *Mechanik, 10*(11), 893-895. DOI: https://doi.org/10.17814/mechanik.2015.11.587.

Piechna, J. (2012). *Podstawy aerodynamiki pojazdów*. Sulejówek: Wydawnictwo WKŁ.

Poole, S., Phillips, R. (2019). Pattern Recognition Association of South Africa and Robotics and Mechat Rapid prototyping of small wind turbine blades using additive manufacturingronics. *International Conference (PRASA-RobMech), 10*, 189-194.

Przydatek, G., Kochanek, A., Basta, M. (2017). Analysis of changes in municipal waste management at the county level. *Journal of Ecological Engineering, 18*(1), 72-80.

Razaviye, M.K., Tafti, R., Khajehmohammadi, A.M. (2022). An investigation on mechanical properties of PA12 parts produced by a SLS 3D printer: an experimental approach CIRP. *J. Manuf. Sci. Technol., 10*(38), 760-768. DOI: https://doi.org/10.1016/j.cirpj.2022.06.016.

Rohl, P.J., Mavris, D.N., Schrage, D.P. (1995). *Combined Aerodynamic and Structural Optimization of a High-Speed Civil Transport Wing*. American Institute of Aeronautics and Astronautics.

Rosso, S., Meneghello, R., Biasetto, L., Grigolato, L., Concheri, G., Savio, G. (2020). In-depth comparison of polyamide 12 parts manufactured by Multi Jet Fusion and Selective Laser Sintering. DOI: https://doi.org/10.1016/j.addma.2020.101713.

Sangeetha, C. (2015). Fluid structure interaction on AGARD 445.6 wing at transonic speeds. *J. Aircr., 10*(2), 28-34.

Somerfield, M. Retrieved from: https://www.motorsport.com/f1/news/analysis-is-f1-set-for-another-flexi-wing-war-777139/777139/2023.

Szczepaniak, R., Lamch, K., Smykla, I. (2015). *The analysis of the possibilities of using the finite element method to determine the impact of the winglet application on aerodynamic characteristics of the glider wing*. In: Proceedings of the Conference on Modelling Fluid Flow the 16th International Conference on Fluid Flow Technologies.

Tomanik, M., Zmudzinska, M., Wojtków, M. (2022). Mechanical and structural evaluation of the PA12 desktop selective laser sintering printed parts regarding printing strategy 3D Print. *Addit. Manuf., 10*(8), 271-280. DOI: https://doi.org/10.1089/3dp.2020.0111.

Tuliszka-Sznitko, E. (2011). *Wybrane zagadnienia z mechaniki płynów wirujących*. Poznań: WPP.

Vreman B., Geurts B., Kuerten, H. (1997). Large eddy simulation of turbulent mixing layer. *Journal of Fluid Mechanics*. DOI: https://doi.org/10.1017/S0022112097005429.

Yu, G., Ma, J., Li, J., Wu, J., Yu, J., Wang, X. (2022). Mechanical and tribological properties of 3D printed polyamide 12 and SiC/PA12 302 composite by selective laser sintering. *Polymers Basel, 10*(14), 2167. DOI: https://doi.org/10.1016/j.eurpolymj.2017.05.014.

Yurkovich, R., (2003). Status of unsteady aerodynamic prediction for flutter of high performance aircraft. *Autobusy – Buses, 10*(40), 832-842. DOI: https://doi.org/10.2514/2.6874.